

Elman 神经网络在表面肌电连续估计肘关节角度中的应用

刘永柏¹, 王刚¹, 柴媛媛¹, 刘克平¹, 金龙², 孙中波¹

(1. 长春工业大学控制工程系 吉林 长春 130000; 2. 兰州大学信息科学与工程学院 甘肃 兰州 730000)

摘要 **目的:** 估计肘关节角度和提高模型的速度和精度。**方法:** 建立并研究基于表面肌电信号 (Surface electromyogram, sEMG) 的 Elman 神经网络 (Elman neural network, ENN), 通过在肱二头肌 (Biceps muscle, BM) 和肱三头肌 (Triceps muscle, TM) 的皮肤表面上放置电极来采集 sEMG 信号, 并通过惯性测量单元 (Inertial measurement unit, IMU) 记录实际的肘关节角度。**结果:** 通过实验结果以及基于模型阶数和隐层神经元数量的参数讨论, 进一步证明了 ENN 可达到的最小均方根 (Root mean square, RMS) 误差为 18.1899 度。**结论:** 在最优的参数下应用 ENN 估计肘关节角度时, 均方根误差达到了可控范围。理论分析和实验结果都证明 ENN 在估计关节角度方面是有效的。

关键词 表面肌电信号; Elman 神经网络; 均方根; 意图识别; 康复

中图分类号 R496 **文献标识码** A **文章编号** 2096-7721 (2021) 04-0295-11

Application of Elman neural network in continuous estimation of elbow joint angle with sEMG

LIU Yongbai¹, WANG Gang¹, CHAI Yuanyuan¹, LIU Keping¹, JIN Long², SUN Zhongbo¹

(1. Department of Control Engineering, Changchun University of Technology, Changchun 130000, China; 2. School of information Science and Engineering, Lanzhou University, Lanzhou 730000, China)

Abstract **Objective:** To estimate the elbow joint angle and improve the rapidity and precision of the model. **Methods:** The elman neural network (ENN) based on surface electromyogram (sEMG) was established and investigated.

收稿日期: 2020-05-17 录用日期: 2020-08-14

Received Date: 2020-05-17 Accepted Date: 2020-08-14

基金项目: 国家自然科学基金项目 (6187330); 中国博士后科学基金项目 (2018M641784, 2019T120240); 吉林省科技发展计划项目 (20200404208YY, 20200201291JC)

Foundation Item: National Natural Science Foundation of China (61873304); China Postdoctoral Science Foundation Project (2018M641784, 2019T120240); Key Science and Technology Projects of Jilin Province, China (20200404208YY, 20200201291JC)

通讯作者: 孙中波, E-mail: zhongbosun2012@163.com

Corresponding Author: SUN Zhongbo, Email: zhongbosun2012@163.com

引用格式: 刘永柏, 王刚, 柴媛媛, 等. Elman 神经网络在表面肌电连续估计肘关节角度中的应用 [J]. 机器人外科学杂志 (中英文), 2021, 2 (4): 295-305.

Citation: LIU Y B, WANG G, CHAI Y Y, et al. Application of Elman neural network in continuous estimation of elbow joint angle with sEMG [J]. Chinese Journal of Robotic Surgery, 2021,2(4):295-305.

The sEMG signals were collected by the electrodes placed on the skin surfaces of biceps muscle (BM) and triceps muscle (TM), and the actual elbow joint angle was recorded by an inertial measurement unit (IMU). **Results:** Theoretical analysis indicates that the ENN is feasible to be employed for estimating the elbow joint angle. Experimental results and the parameter discussion based on the model order and the number of hidden layer neurons further indicate that the minimum RMS error of ENN is 18.1899 degree. **Conclusion:** The RMS error is controllable when the ENN is used to estimate the elbow joint angle under the optimal parameter. Theoretical analysis and experimental results shows that the ENN is effective in estimation of joint angles.

Key words sEMG; Elman neural network; RMS; Intention recognition; Rehabilitation

With the population aging in China, the number of physical disabilities caused by stroke, spinal cord injury, brain trauma and other reasons has increased rapidly. Among them, stroke is the main disease that gives rise to local skeletal muscle dysfunction in the upper limbs^[1]. At present, the main treatment methods are physical therapy and robotic rehabilitation way. With the rapid development of robots in the medical, military, industrial and other neighborhoods^[2-4], the rehabilitation robot therapy will become simpler and more efficient. Human-computer interaction control method and active motion intention recognition are two core techniques in the field of rehabilitation robot research^[5-7].

Human motion intentions are generated in the brain and transmitted to joint motion through multiple complex neural subsystems. It requires the upper limb rehabilitation robots to collect human biological signals and recognize human motion intentions accurately. Specifically, the biological signals usually include electroencephalogram (EEG), electrooculogram (EOG), electromyography (EMG) and mechanical signals^[8-12]. In recent years, there are many methods, such as support vector machine (SVM)^[13], the Hill-based muscle model^[14-15] and state-space models^[15-16], to be applied to estimate the motion intention. Although a few algorithms have been developed to estimate the

human motion intentions based on the EEG, EOG and EMG, the existing models still have room for improvement in data acquisition, data processing, prediction accuracy and stability. Therefore, researching on the data processing, accuracy and rapidity of algorithms still have a wide range of significance. In this paper, the ENN will be established to estimate the elbow joint angle of one able-bodied subject. The theoretical analysis and experiments indicate the superior performance of the model.

With the widespread application of neural networks in the fields of science and engineering^[17-21], many neural networks have been employed in the recognition of human-computer interaction. A back propagation neural network (BPNN) was established to estimate the joint angles of hip, knee, and ankle from the sEMG signals^[22]. Analogously, Aung Y M et al. designed the BP neural network to predict the joint angles of shoulder and elbow using sEMG signals^[23]. An artificial neural network of radial basis function (RBFNN) was developed to estimate the joint angles of hip, knee, and ankle from the sEMG signals of rectus femoris, lateral femoral muscle and extensor hallucis^[24]. As a contrast, both BPNN and RBFNN are static feedforward neural networks, although the BPNN is simpler in structure than RBFNN, the stationary learning rate and unstable learning and

memory ability will make BPNN inferior to RBFNN in training rate and adaptive ability. However, ENN, a kind of dynamic recursive neural network, has increased the receiving layers to maintain the advantages of short-term memory, rapid training rate and strong network stability^[25].

In this paper, the ENN is developed to estimate the elbow joint angle. Firstly, the sEMG signals of BM and TM was collected from an able-bodied subject by the angle sensor IMU and biopac system, then, the raw sEMG signals was processed by high-pass filter and low-pass filter to remove unnecessary noise. Additionally, the order of model and the number of hidden layer neurons were discussed to obtain the optimal parameters, which could guarantee the optimal performance of the model during the neural network training. Ultimately, the evaluation index RMS error of the model would further indicate the excellent performance of the ENN in estimating the elbow joint angle.

1 Experimental procedures and methods

1.1 Data acquisition

To acquire more accurate experimental data, a healthy subject (female, 26 years old) was selected to participate in the arm flexion and extension exercise experiment in this experiment. According to DING Q[©] et al.^[16], the elbow joint of the arm mainly passed through the BM (stretching/contraction) and TM (stretching/contraction) to achieve flexion and extension. Therefore, the effective sEMG signals to be collected in this experiment are mainly from BM and TM. In addition, the IMU module should be attached to the forearm and rotated around the x-axis to collect the joint angle of the elbow joint. The experimental procedures and equipment are shown in Figure 1 and Figure 2. The testing process basically includes the following steps:

- a. Clean BM and TM with alcohol, then attach

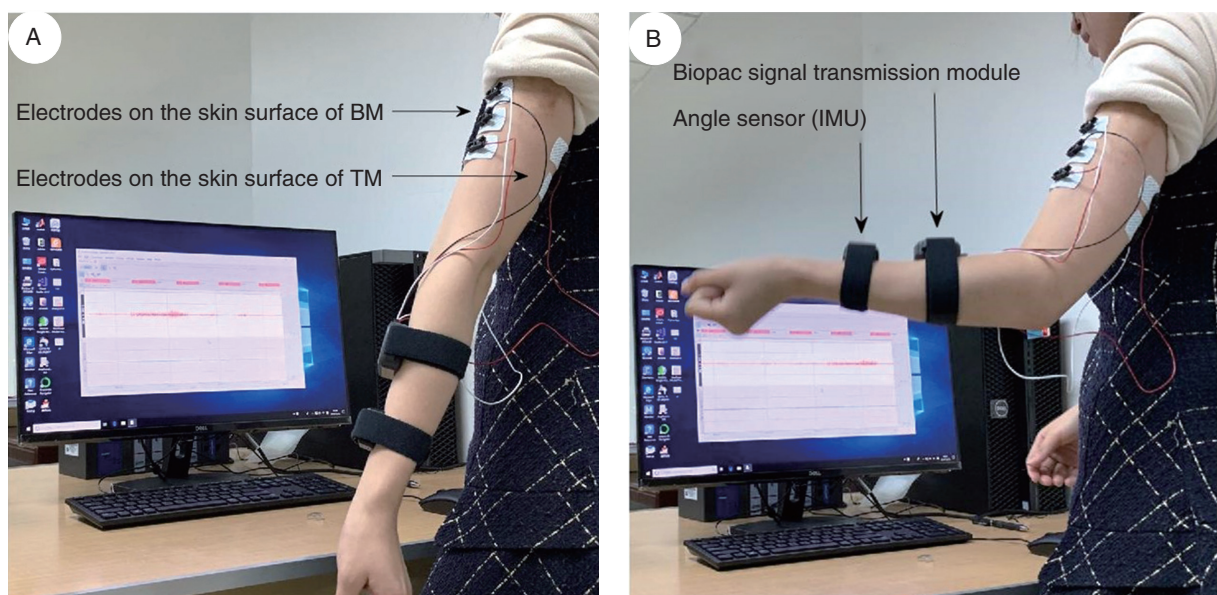


Figure 1 Data acquisition during the arm (flexion/extension) experiment
A. Arm extension experiment; B. Arm flexion experiment.

electrodes to skin surfaces of BM and TM.

b. Bind the angle sensor IMU and the Biopac signal transmission module to the subject's arm, then, connect the Biopac signal transmission module with the electrode pad. At the same time, the Biopac signal transmitting module and the Biopac signal receiving module shall be connected successfully. The IMU and Biopac signal transmission modules are shown in Figure 2.

c. Open MiniIMU and Biopac signal acquisition system on the computer for synchronous data acquisition of elbow joint angle signal and sEMG signal.

Since the collection of sEMG signals could be affected by sweat, body temperature and so on. The skin surfaces of the BM and TM shall be cleaned to reduce the distortion on data. In addition, three disposable electrode slices shall be attached on the skin surfaces of the BM and TM in this experiment. Specially, the distance between each pair of electrodes is 2~3cm. After the above operations, the data recorded during the arm flexion and extension experiments can be obtained as shown in Figure 3.

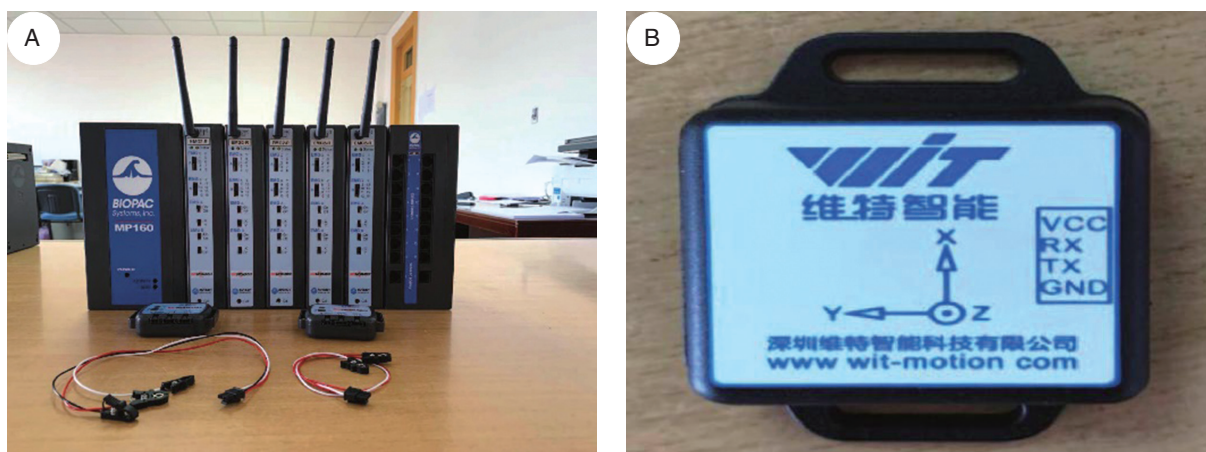


Figure 2 The angle sensor IMU and the Biopac signal transmission module
A. Biopac signal transmission module; B. IMU.

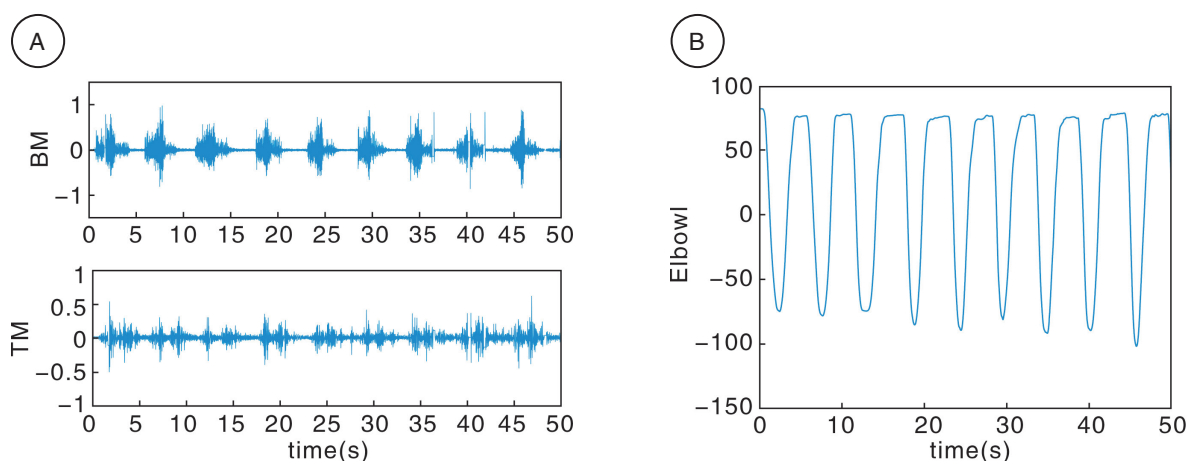


Figure 3 The subjects' data recorded during arm flexion and extension experiments
A. Raw sEMG signals; B. Elbow joint angle.

1.2 Signals processing

This study finds that the sEMG signals and elbow joint angle change regularly with arm flexion and extension in Figure 3. Nevertheless, the raw sEMG signals of BM and TM are contaminated by noises during data acquisition. Generally speaking, the noises may be derived from the inherent noise of the equipment, the test environment, and the electromagnetic environment. Among them, the inherent noise of equipment usually includes 50Hz industrial frequency noise, DC bias et al. The noise in the testing environment principally comes from the sweat of the skin, body hair and temperature. Similarly, considering the signal transmitters of Biopac equipment utilize wireless transmission devices for information transmission. Therefore, in order to avert electromagnetic interference between cables and wireless signals, the IMU wired sensors are employed to supersede the wireless to reduce electromagnetic interference between wireless devices.

Boxtel thinks it can be obtained that the effective frequency of the above raw sEMG signal is 0~500Hz^[26]. Taking into account that an industrial frequency of 50Hz and the frequency range of 0~20Hz generated by the motor unit^[27]. Therefore, a high-pass filter with a cut-off frequency of 500Hz is utilized to eliminate high frequencies above 500Hz, and a low-pass filter with a cut-off frequency of 20Hz is employed to remove the interference frequency range of 0~20Hz in the course of signal processing. Meanwhile, the industrial frequency of 50Hz needs to be taken out by a notch filter with cut-off frequency of 50Hz.

Although an effective sEMG signal can be obtained after filtering the raw sEMG signal, the amplitude of the processed signal will oscillate frequently. Therefore, the signals need to be further processed by the full-wave rectification, and the formula can be described as following.

$$sEMG_r(n) = |sEMG_p(n)| \quad (1)$$

Where $sEMG_p(n)$ is the n th amplitude of the processed sEMG signals, $sEMG_r(n)$ is the n th amplitude sample of the sEMG signals obtained after full-wave rectification.

It's worth pointing out that the sampling frequency of sEMG signals is 2kHz, and the sampling frequency of the elbow joint angle is 100Hz. Therefore, in order to keep the sampling frequency of both, the sEMG signals are sub-sampled to match the sampling frequency of elbow joint angle, and the sub-sampled process can be expressed as

$$sEMG_s(n) = \frac{1}{N} \sum_{i=nN-N+1}^{nN} sEMG_r(i) \quad (2)$$

Where N is the number of sub-sampling, and $sEMG_s(n)$ is the sEMG signals after sub-sampling.

After the above signal processing, the processed signals of sEMG can be shown as Figure 4.

1.3 ENN establishment

Suppose that, the data acquired during the arm flexion and extension experiment can be described as follows.

$$\begin{cases} \theta = [\theta_1, \dots, \dots, \theta_j, \dots, \theta_t] & t = 5000 \\ a_i = [a_{i,1}, \dots, a_{i,j}, \dots, a_{i,t}] & t = 1, \dots, k \end{cases} \quad (3)$$

Where θ is the elbow joint angle measured by IMU, a_i signifies the processed sEMG signals of BM and TM, and the k represents the channel number of Biopac equipment. Since the sEMG signals collected from BM and TM, the channel number is 2 in the

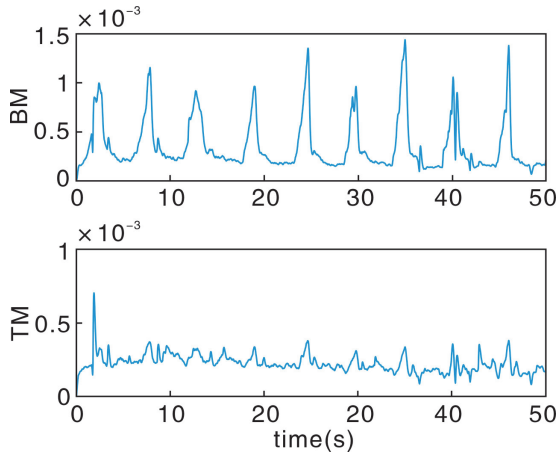


Figure 4 The sEMG signals of BM and TM after signal processing

experiment. As shown in Figure 3, the amplitude of the sEMG signal increases with muscle contraction, and the elbow joint angle changes with the muscle contraction or stretching. Since the relationship between muscle (contraction/stretching) and sEMG signals is nonlinear, the relationship between joint angle and sEMG signals can be regarded as nonlinear. The nonlinear function can be expressed as follows.

$$\theta_e(i) = F(a_{1,i}, \dots, a_{1,i-m+1}; a_{2,i}, \dots, a_{2,i-m+1}; a_{k,i}, \dots, a_{k,i-m+1}) \quad i=m, \dots, t \quad (4)$$

Where $\theta_e(i)$ is the elbow joint angle estimated by the model at the i th time, F signifies the undetermined nonlinear function, and m denotes the order of the model.

In this paper, ENN, a typical dynamic recurrent neural network, is established to estimate the elbow joint angle. As can be seen from Figure 5–A, the structure of ENN comprises four parts that input layer, hidden layer, receiving layer and output layer. Compared with BPNN, receiving layer was added to ENN to memorize the output value of the hidden layer unit at the previous moment and return it to the input of ENN. The structure of ENN will increase the

sensitivity of the network to historical data, so that the dynamic information can be better processed.

The state space expression of ENN can be described as follows.

$$\begin{cases} \theta_e(k) = \Phi(\omega_3 x(k)) \\ x(k) = \Psi(\omega_1 x_c(k) + \omega_2 u(k-1)) \\ x_c(k) = x(k-1) \end{cases} \quad (5)$$

Where θ_e is the elbow joint angle estimated by the ENN, x denotes the intermediate layer node unit vector, u represents the input vector and x_c for the feedback state vector. In addition, ω_1 , ω_2 and ω_3 are respectively the weights coefficient from the receiving layer to the hidden layer, the input layer to the hidden layer and the hidden layer to the output layer. $\Phi(\cdot)$ and $\Psi(\cdot)$ represent the transfer functions of the output layer neurons and the hidden layer neurons respectively.

In this experiment, the inputted a_i is a matrix consisted of the processed signals of BM and TM, and the number of the input layer neurons depends on the number of muscles and the order of the model. The number of muscles to be collected is 2 and the model order m is uncertain, the number of the input layer neurons is $k=2*m$. Similarly, the number of hidden layer neurons n is also variable, and the output of ENN is elbow joint angle. During the ENN training, the first 5000 times of processing sEMG signals of the BM and TM are utilized for experiments, of which the first 2500 times were served as training and the last 2500 times as testing. Ultimately, in order to better evaluate the performance of the model, the RMS error is used to evaluate the accuracy of the model, which can be expressed as follows.

$$\text{RMS} = \sqrt{\frac{\sum_{i=1}^{2500} (\theta(i) - \theta_e(i))^2}{2500}} \quad (6)$$

Where $\theta(i)$ denotes the actual elbow joint angle measured by the IMU.

Hereto, the subsections of data acquisition, signals processing and ENN establishment have been introduced in the section of experimental and method. In order to better explain the prediction process, the experimental process, learning and training process of ENN can be shown as Figure 5-B.

2 Results and discussion

In this section, the ENN is applied for the estimation of elbow joint angle, it is worth mentioning that an appropriate m and n are significant for the elbow joint angle estimation. Therefore, an optimal number of hidden layer neurons n and order m need to be selected to achieve the accurate estimation of elbow joint angle by ENN.

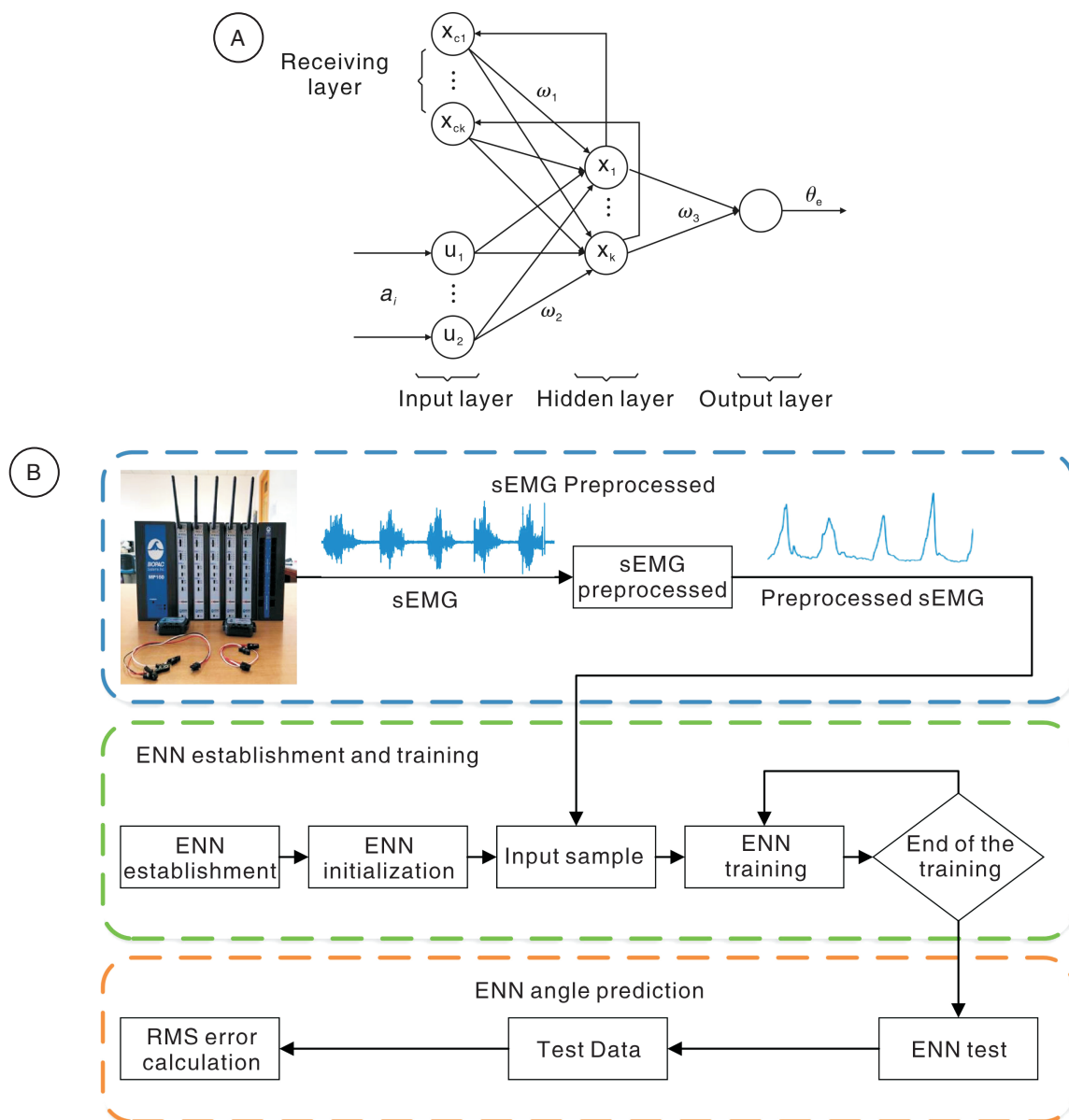


Figure 5 The schematic diagram of ENN
A. Algorithm structure of ENN; B. Algorithm flowchart of ENN.

2.1 Discussion on parameters

From a quantitative perspective, $m=10, 20, \dots, 60$ and $n=10, 20, \dots, 100$ will be taken into account to acquire the optimal number of hidden layer neurons and the order in the ENN training process. The RMS error of ENN with different number of hidden layer neurons and different order can be seen in Figure 6 and Table 1.

The ENN achieves the optimal performance when the number of hidden layer neurons $n=60$ and the order $m=40$ (Figure 6–A). Since the model has achieved the optimal performance at $m=40$, hence, the figures of RMS error with different m are omitted here. Additionally, the RMS error is smallest at $n=60$ and $m=40$ (Figure 6–B). It indicates that choosing an appropriate m and n is an important step to estimate elbow joint angle with ENN. For better comparison, the RMS error value of ENN with different m and n are listed in the Table 1. As we can see from Figure 6

and Table 1 that the minimum RMS error is 18.1899 degree at $m=40$ and $n=60$.

2.2 Model comparison and result analysis

After selecting the optimal number of hidden layer neurons at $n=60$ and the order $m=40$. Subsequently, the ENN estimation of elbow joint angle can be seen in Figure 7–A. The estimated elbow joint angle (EEJA) tracks the actual elbow joint angle (AEJA) smoothly (Figure 7–A). In addition, the Minimum RMS error is 18.1899 and the optimal time is 9.3034s in Table 2. Therefore, the experimental results have proved that ENN is successful and effective in elbow joint angle estimation.

In order to further demonstrate the superiority of ENN in data prediction, the RBFNN and BPNN are used to estimate the elbow joint angle for comparison. The optimal parameters m and n have been discussed in the estimation of joint angles^[22, 24]. Therefore, to save layout space, the discussion of the parameters

Table 1 The RMS error of elbow joint angle estimation with different number of hidden layer neurons and different order

n	RMS					
	$m=10$	$m=20$	$m=30$	$m=40$	$m=50$	$m=60$
10	30.069 8	25.121 2	33.609 0	28.593 9	26.597 5	34.348 1
20	29.203 0	23.846 7	22.584 1	21.466 9	24.974 4	22.889 0
30	25.172 7	23.188 4	22.279 1	19.891 0	23.678 6	25.316 0
40	25.453 1	25.020 0	21.081 9	20.732 6	21.211 0	22.124 0
50	24.716 1	22.797 5	19.184 5	19.563 0	20.226 2	21.512 8
60	25.184 5	22.484 1	20.123 1	18.189 9	21.491 3	21.679 7
70	26.622 2	23.224 0	21.193 0	21.164 1	20.702 6	20.872 6
80	26.404 9	21.089 6	19.339 8	19.758 4	20.501 2	21.661 7
90	28.224 4	20.454 4	20.353 1	20.526 5	21.455 5	21.031 2
100	25.674 0	22.110 7	20.817 3	20.571 5	21.020 4	21.343 7

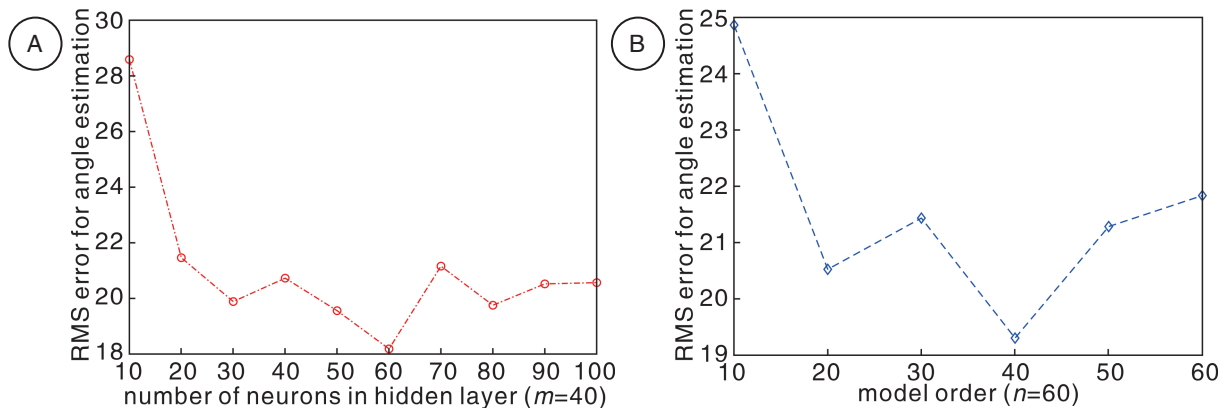


Figure 6 The RMS errors of ENN with different m and n during the arm (flexion/extension) exercise for one able-bodied subject

A. RMS error of ENN with $m=40$ and different n ; B. RMS error of ENN with $n=60$ and different m .

of the RBFNN and BPNN in estimating the elbow joint angle are omitted here. It is worth noting that the optimal parameters $m=20$ and $n=20$ are selected for elbow joint angle estimation with BPNN and RBFNN. The elbow joint angle estimated by RBFNN can be seen in Figure 7-B, and the elbow joint angle estimation of BPNN is shown in Figure 7-C.

According to the Figure 7 and Table 2, it can be summarized that the RBFNN and BPNN can also be used to estimate the elbow joint angle, but ENN is superior to RBFNN and BPNN in accuracy.

Table 2 Comparisons between time and RMS error with ENN, RBFNN and BPNN

	ENN	RBFNN	BPNN
time(s)	9.303 4	9.477 1	7.326 1
RMS(degree)	18.189 9	21.067 6	21.476 6

3 Conclusions

In this paper, based on the sEMG signals of BM and TM, the ENN has been established, analyzed and investigated on estimating the elbow joint angle.

Experimental results have testified that the proposed model is efficient in estimating the elbow joint angle. It is worth mentioning that signal processing and discussion on parameters m and n are still crucial part in the experiment. The raw sEMG signals need to be processed and sub-sampled to get a series of available signal that can be used as input of the ENN. After some experiments and comparisons, it can be obtained from Figure 6, Figure 7-A and Table. I that the ENN revealed the optimal performance at $m=40$ and $n=60$, and the minimum RMS error is 18.1899 degree. So far, all theoretical analysis and experimental results proved that the ENN is effective in estimating joint angles.

For the future direction, the spinal cord injury and stroke patients will be invited to take part in the data acquisition, then, multiple joint angles including shoulders, elbows and wrists will be estimated by the ENN. In addition, the ENN can also be applied to predict the joint angles of lower limbs including hips, knees and ankles.

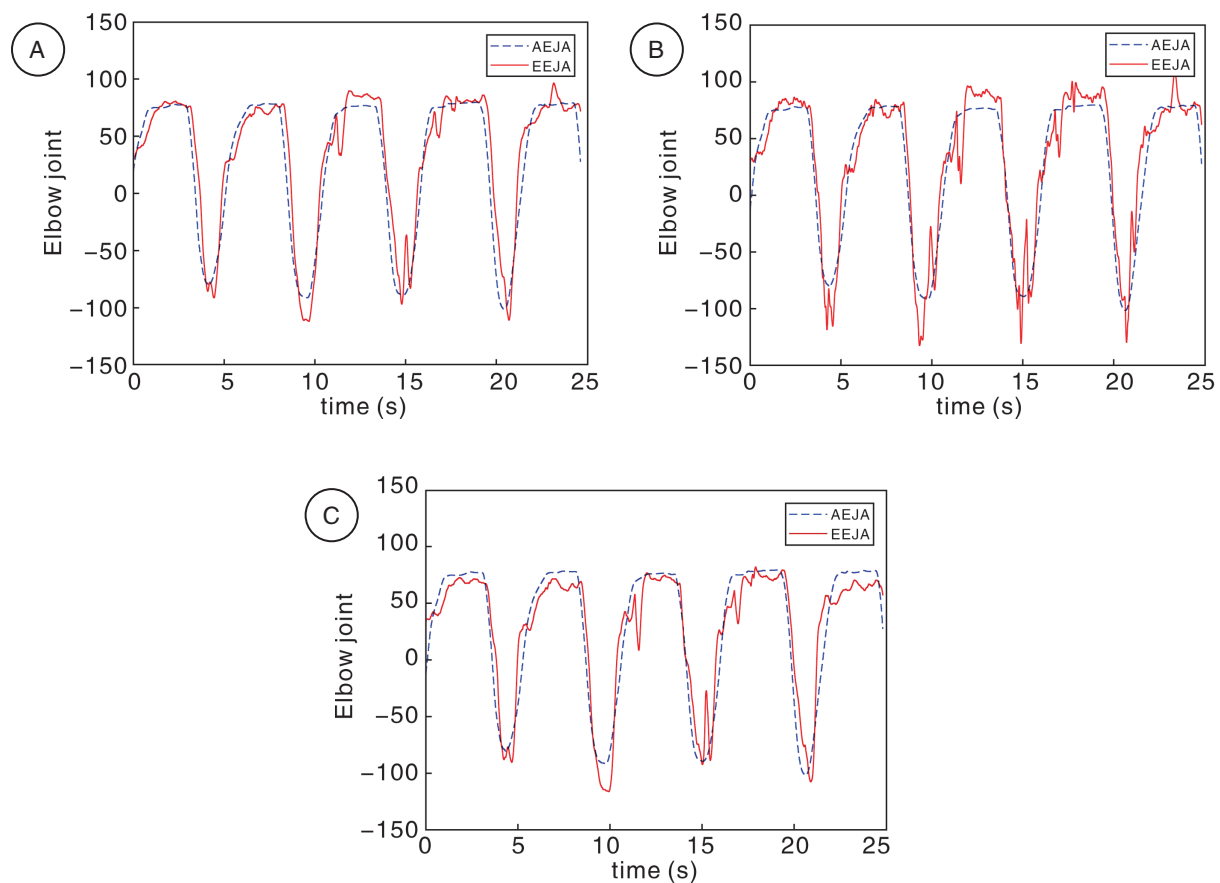


Figure 7 The predicted value of human upper limb elbow joint angle obtained from different models
 A. ENN with $m=40$ and $n=60$; B. RBFNN with $m=20$ and $n=20$; C. BPNN with $m=20$ and $n=20$.

References

- [1] Zorowitz R D, Gillard P J, Brainin M. Poststroke spasticity: sequelae and burden on stroke survivors and caregivers[J]. *Neurology*, 2013, 80(3): S45–S52.
- [2] ZHANG Z J, ZHENG L N, YU J M, et al. Three recurrent neural networks and three numerical methods for solving a repetitive motion planning scheme of redundant robot manipulators[J]. *IEEE-ASME Trans Mechatron*, 2017, 22(3): 1423–1434.
- [3] JIN L, LI S, LUO X, et al. Neural dynamics for cooperative control of redundant robot manipulators[J]. *IEEE Trans Ind Informat*, 2018, 14(9): 3812–3821.
- [4] YANG C, GUO S X, BAO X Q, et al. A vascular interventional surgical robot based on surgeons operating skills[J]. *Med Biol Eng Comput*, 2019, 57(3): 1999–2020.
- [5] Kim Y M, Koo S Y, Lim J G, et al. A robust online touch pattern recognition for dynamic human-robot interaction[J]. *IEEE Trans. Consum. Electron.*, 2010, 56(3): 1979–1987.
- [6] LI Z J, SU C Y, LI G L, et al. Fuzzy approximation-based adaptive backstepping control of an exoskeleton for human upper limbs[J]. *IEEE Trans Fuzzy Syst*, 2015, 23(3): 555–566.
- [7] Han J H, Lee S J, Kim J H, et al. Behavior hierarchy-based affordance map for recognition of human intention and its application to human-robot interaction[J]. *IEEE Trans Hum-Mach Syst*, 2016, 46(5): 708–722.
- [8] Nam Y, Koo B, Cichocki A, et al. GOM-Face: GKP, EOG, and EMG-based multimodal interface with application to humanoid robot control[J]. *IEEE Trans Biomed. Eng.*, 2013, 61(2): 453–462.
- [9] Kumar S, Sharma A. A new parameter tuning approach

- for enhanced motor imagery EEG signal classification[J]. *Med Biol Eng Comput*, 2018, 56(10): 1861–1874.
- [10] DUAN F, DAI L L, CHANG W N, et al. SEMG-based identification of hand motion commands using wavelet neural network combined with discrete wavelet transform[J]. *IEEE Trans Ind Electron*, 2015, 63(3): 1923–1934.
- [11] LIU Y J, LI J, TONG S, et al. Neural network control-based adaptive learning design for nonlinear systems with full-state constraints[J]. *IEEE Trans Neural Netw Learn Syst*, 2016, 27(7): 1562–1571.
- [12] Artemiadis P K, Kyriakopoulos K J. An EMG-based robot control scheme robust to time-varying emg signal features[J]. *IEEE T Inf Technol B*, 2010, 14(3): 582–588.
- [13] SHI J, ZHENG Y P, YAN Z Z. SVM for estimation of wrist angle from sonomyography and sEMG signals[C]. *IEEE International Conference on EMBS*, 2007: 806–4809.
- [14] Hill A V. The heat of shortening and the dynamic constants of muscle[J]. *Proc. of Royal Society of London, Series B*, 1938, 126(843): 136–195.
- [15] HAN J D, DING Q C, XIONG A B, et al. A state-space EMG model for the estimation of continuous joint movements[J]. *IEEE Trans Ind Electron*, 2015, 62(7): 4267–4275.
- [16] DING Q C, HAN J D, ZHAO X G. Continuous estimation of human multi-joint angles from semg using a state-space model[J]. *IEEE Trans Neural Syst Rehabil Eng*, 2016, 25(9): 1518–1528.
- [17] XIA Y S, FENG G, WANG J. A primal-dual neural network for online resolving constrained kinematic redundancy in robot motion control[J]. *IEEE Trans Cybern*, 2005, 35(1): 54–64.
- [18] JIN L, LI S, LIN B L, et al. Zeroing neural networks: a survey[J]. *Neurocomputing*, 2017, 267(6): 597–604.
- [19] JIN L, LI S, YU J G, et al. Robot manipulator control using neural networks: a survey[J]. *Neurocomputing*, 2018, 285(12): 23–24.
- [20] SUN Z B, LI F, ZHANG B C, et al. Different modified zeroing neural dynamics with inherent tolerance to noises for time-varying reciprocal problems: A control-theoretic approach[J]. *Neurocomputing*, 2019, 337: 165–179.
- [21] SUN Z B, LIU Y B, WEI L, et al. Two dtznn models of $O(\tau^2)$ pattern for online solving dynamic system of linear equations: application to manipulator motion generation[J]. *IEEE Access*, 2020, 8: 36624–36638.
- [22] ZHANG F, LI P F, HOU Z G, et al. sEMG-based continuous estimation of joint angles of human legs by using BP neural network[J]. *Neurocomputing*, 2012, 78(1): 139–148.
- [23] Aung Y M, Al-jumail Y A. Estimation of upper limb joint angle using surface EMG signal[J]. *Int J Adv Robot Syst*, 2013, 10(369): 1–8.
- [24] WANG G, LIU Y B, SHI T, et al. A novel estimation approach of semg-based joint movements via RBF neural network[C]. *2019 Chinese Automation Congress*, 2020: 2059–2064.
- [25] GAO X Z, GAO X M, Ovaska S J. A modified Elman neural network model with application to dynamical systems identification[C]. *IEEE International Conference on Systems*, 1996: 1376–1381.
- [26] Bostel A, Boelhauer A J W, Bos A R. Optimal EMG signal bandwidth and interelectrode distance for the recording of acoustic, electrocutaneous, and photic blink reflexes[J]. *Psychophysiology*, 1998, 35(6): 690–697.
- [27] Christie A, Greig Inglis J, Kamen G, et al. Relationships between surface EMG variables and motor unit firing rates[J]. *Eur J Appl Physiol*, 2009, 107(2): 177–185.